654 | https://doi.org/10.3311/PPci.43182
Creative Commons Attribution

Periodica Polytechnica Civil Engineering, 70(2), pp. 654–667, 2026

Near-real-time Probabilistic Assessment of Riverbank Structures using Monitoring-integrated Numerical Models

Shiji Ma[1], Lan Qiao[2], Meng Zhang[3], Ruizhi Wang[4*], Qingwen Li[2], Jianhong Man[2]

[1] School of Future Cities, University of Science and Technology Beijing, No. 30 Xueyuan Road, Haidian District, 100083 Beijing, China
[2] School of Resources and Safety Engineering, University of Science and Technology Beijing, No. 30 Xueyuan Road, Haidian District, 100083 Beijing, China
[3] China First Highway Engineering Co., Ltd., Block A, Shitong International Building, Zhoujiajing, Guanzhuang, Chaoyang District, 100024 Beijing, China
[4] Center for School Development and Planning, Ministry of Education, 15th Floor, Science and Technology Building, No. 3 Shangyuancun, Haidian District, 100044 Beijing, China
* Corresponding author, e-mail: wangruizhi1992c@163.com

Received: 26 December 2025, Accepted: 27 April 2026, Published online: 17 June 2026

Abstract

Riverbank hydraulic structures are typically monitored using deterministic thresholds, whereas their reliability is assessed through probabilistic analysis during design. This separation limits the ability of monitoring systems to quantify evolving structural risk under uncertain geotechnical conditions and stochastic excitations. To bridge this gap, this study proposes an integrated probabilistic monitoring framework that couples offline probability density evolution (PDEM) with online surrogate-based distribution correction. An offline baseline database of response probability density surfaces (PDS) is established by incorporating spatially variable geotechnical parameters and stochastic excitation models within a reduced-dimensional representation. This baseline captures the temporal evolution of structural response distributions under representative environmental scenarios. For near-real-time application, a lightweight surrogate model is developed to infer distribution-level correction parameters from monitoring-derived features, enabling rapid reconstruction of updated PDS without repeated dynamic simulations. The framework is validated through a numerical case study of a Π-shaped anti-scour wall slope. The surrogate-reconstructed PDS demonstrates strong agreement with direct probabilistic solutions, with Jensen-Shannon divergence and Earth Mover's Distance generally below 0.1, while reducing computational cost by more than two orders of magnitude. The proposed method enables real-time extraction of distribution-based risk indicators and provides a probability-informed pathway for monitoring and early warning of hydraulic structures subjected to coupled environmental uncertainties.

Keywords

probabilistic monitoring, probability density evolution, surrogate modelling, spatial variability, hydraulic structures

1 Introduction

Hydraulic structures, such as riverbank protection systems and anti-scour walls, play an essential role in slope stabilization and urban flood control. Their performance is influenced by multiple sources of uncertainty, including stochastic hydraulic loading, seismic disturbances, seepage pressure variation, and spatial variability of geotechnical properties. Recent studies have emphasized the stochastic characteristics of bank erosion and hydraulic-geotechnical interactions under complex environmental conditions [1–2]. Soil heterogeneity in grain size distribution, moisture content, and compaction state, together with construction variability and ageing effects in concrete materials, further increase uncertainty. Stochastic seepage processes and spatial variability of soil parameters significantly affect structural reliability [3–4]. Consequently, the structural response of hydraulic systems should be treated as a stochastic process rather than a deterministic quantity. Probabilistic structural analysis therefore aims to characterize the evolution of response distributions under uncertain inputs and support risk-informed evaluation. Time-dependent reliability analysis has been widely applied to flood defence systems [5–6]. However, practical monitoring in hydraulic engineering still relies largely on deterministic thresholds or empirical indicators, which cannot fully represent distributional characteristics or extreme-response risks under coupled excitations.

Cite this article as: Ma, S., Qiao, L., Zhang, M., Wang, R., Li, Q., Man, J. "Near-real-time Probabilistic Assessment of Riverbank Structures using Monitoring-integrated Numerical Models", Periodica Polytechnica Civil Engineering, 70(2), pp. 654–667, 2026. https://doi.org/10.3311/PPci.43182

Considerable efforts have been devoted to uncertainty propagation in structural and geotechnical systems. Sampling-based approaches, including Monte Carlo simulation and stochastic finite element methods, provide general tools for mapping input randomness to response distributions [7]. Efficiency improvements such as Latin hypercube sampling and quasi-Monte Carlo simulation have been proposed to reduce computational cost [8]. Surrogate modelling techniques are frequently constructed offline to approximate complex input-response relationships and accelerate probabilistic estimation. Nevertheless, high-dimensional random fields arising from spatially variable material properties and multiscale processes lead to rapid growth in computational demand. For nonlinear dynamic problems, repeated simulations remain computationally intensive, limiting real-time applicability.

The Probability Density Evolution Method (PDEM) offers a density-based alternative for uncertainty propagation by solving governing equations in probability space [9–10]. Instead of estimating only statistical moments, PDEM tracks the complete probability density function of structural responses, enabling explicit representation of mean, variance, and higher-order characteristics. Applications to seismic assessment of earth-retaining structures have demonstrated its capability in capturing nonlinear stochastic responses [11–12]. However, large-scale engineering implementation is challenged by the dimensionality of random inputs. Three-dimensional spatial random fields often require discretization into numerous random variables, resulting in substantial computational burden. Advanced formulations of generalized density evolution equations further extend theoretical capability but increase modelling complexity [13–14]. Effective dimensionality reduction is therefore necessary to preserve dominant uncertainty modes while maintaining computational feasibility.

Advances in multi-source sensing technologies have enabled continuous monitoring of hydraulic structures. Modern monitoring networks acquire displacement, acceleration, pore pressure, strain, and inclination data from both structural and geotechnical components. Data fusion and system identification techniques have been widely studied in structural health monitoring [15–16]. Bayesian surrogate modelling and adaptive updating strategies have also shown potential for probabilistic data assimilation [17]. In practical hydraulic applications, however, monitoring data are primarily used for threshold-based alarms or empirical indicators. The probabilistic information contained in monitoring data and its role in updating response distributions in real time have received limited attention. An integrated framework is therefore required to combine probabilistic baseline modelling with monitoring-driven updating mechanisms, enabling rapid reconstruction of response probability distributions while preserving physical interpretability.

Despite progress in uncertainty quantification and monitoring technologies, several challenges remain. First, probabilistic analysis and structural monitoring are often treated separately, and few studies establish a unified framework linking offline density evolution with online probabilistic updating. Second, high-dimensional spatial variability restricts the application of density-based evolution methods in large-scale hydraulic systems. Third, efficient inference mechanisms capable of adjusting probabilistic baselines using real-time monitoring data without repeated dynamic simulations are still lacking. Addressing these issues is essential for probability-informed monitoring and early warning under complex environmental conditions.

To address the above challenges, this study proposes a probabilistic monitoring and early-warning framework for anti-scour wall slopes that integrates offline probability density evolution with online surrogate-based correction. An offline database of response probability density surfaces is first established using stochastic excitation modelling and reduced-dimensional representation of spatially variable geotechnical parameters. A lightweight surrogate model is then developed to infer distribution-level correction parameters from monitoring-derived features, enabling rapid reconstruction of updated probability density surfaces without repeated dynamic analysis. The main contributions are summarized as follows:

An integrated offline-online probabilistic monitoring framework linking density evolution analysis with real-time structural monitoring.

A reduced-dimensional uncertainty representation strategy tailored to probability density evolution modelling.

A surrogate-based distribution reconstruction approach that enables near-real-time probabilistic updating with improved computational efficiency.

The proposed framework provides a probability-informed approach for monitoring, risk assessment, and early warning of hydraulic structures subjected to coupled environmental uncertainties.

2 Theoretical backgrounds

2.1 Probability density evolution method

The PDEM originates from stochastic dynamical system theory. Its core idea is to propagate input uncertainties to

output responses by solving the time evolution of the system response's probability density function (PDF) [18–19]. Considering a slope subject to stochastic vibration and modeled with random parameters, let the m-dimensional vector of quantities of interest be defined as $\boldsymbol{Z} = (Z_1, Z_2, \ldots, Z_m)^T$. The system dynamics can then be described by the following form [20]:

$$\boldsymbol{M}(\Theta)\ddot{\boldsymbol{X}} + \boldsymbol{f}\left(\dot{\boldsymbol{X}}, \boldsymbol{X}, \Theta\right) = \Gamma \boldsymbol{F}(\Theta, t) \tag{1}$$

$$\boldsymbol{Z} = \boldsymbol{Z}(\theta, t) = \boldsymbol{H}_{\boldsymbol{Z}}(\Theta, t) = \boldsymbol{L}(\boldsymbol{X}, \Theta, t) \tag{2}$$

In Eq. (1) and Eq. (2), $\Theta = \{\theta_1, \theta_2, \ldots, \theta_s\} \in \boldsymbol{R}^s$ denotes the set of fundamental random variables representing uncertainties in structural parameters and excitations. $\boldsymbol{X} = \boldsymbol{H}(\Theta, t)$ represents the n-dimensional displacement response vector of the system, $\boldsymbol{M}$ represents the $n \times n$ mass matrix, $\boldsymbol{f}$ represents the n-dimensional internal force vector incorporating nonlinearities, Γ represents the $n \times r$ excitation influence matrix, $\boldsymbol{F}$ represents the r-dimensional excitation vector. The operator $\boldsymbol{H}_{\boldsymbol{Z}}$ defines the quantities of interest, $\boldsymbol{H}$ is the displacement operator, $\boldsymbol{L}$ maps the system response $\boldsymbol{X}$ to the m-dimensional vector of quantities of interest $\boldsymbol{Z}$.

The joint probability density function of ($\boldsymbol{Z}$, Θ), denoted as $p_{z\Theta}(z, \theta, t)$, then satisfies the generalized probability density evolution equation (GDEE):

$$\frac{\partial p_{\boldsymbol{Z}\Theta}(z,\theta,t)}{\partial t} + \sum_{l=1}^{m} \dot{Z}_l(\theta,t) \frac{\partial p_{\boldsymbol{Z}\Theta}(z,\theta,t)}{\partial z_l} = 0 \tag{3}$$

In Eq. (3), $\dot{Z}_l$ denotes the generalized velocity of the l-th quantity of interest.

Accordingly, the joint PDF of $\boldsymbol{Z}$ can be expressed as:

$$p_{\boldsymbol{Z}}(z,t) = \int_{\Omega_\Theta} p_{\boldsymbol{Z}\Theta}(z,\theta,t)\, d\theta \tag{4}$$

In Eq. (4), Ω_Θ denotes the space composed of the set of random variables Θ.

2.2 Karhunen-Loève expansion

Geotechnical parameters of hydraulic structure systems, such as elastic modulus, internal friction angle and permeability, often exhibit spatial correlation. Their variability is reflected not only in the mean and variance but also in spatial dependence [21–22]. Directly discretizing these random fields in numerical simulations would lead to a high-dimensional uncertainty input, making probabilistic propagation analysis computationally intractable. To retain the ability to characterize spatial correlation while controlling the dimensionality of randomness, this study employs the KLE to construct a reduced order representation of the random fields [23–24].

Let the spatial distribution of a parameter be modeled as a random field $G(\boldsymbol{x}, \omega)$ defined over the spatial domain $\Omega_G \in \boldsymbol{R}^3$, where $\boldsymbol{x} = (x, y, z)$ denotes the spatial position and ω represents a random event in the sample space. The statistical properties of this random field are characterized by its mean function $\mu_G(\boldsymbol{x})$ and covariance function $C_G(\boldsymbol{x}, \boldsymbol{x}')$, defined as [25–26]:

$$\begin{cases} \mu_G(\boldsymbol{x}) = E\left[G(\boldsymbol{x},\omega)\right] \\ C_G = E\left[\left(G(\boldsymbol{x},\omega) - \mu_G(\boldsymbol{x})\right)\left(G(\boldsymbol{x}',\omega) - \mu_G(\boldsymbol{x}')\right)\right] \end{cases} \tag{5}$$

In Eq. (5), $E[\cdot]$ denotes the expectation over the sample space, $C_G = C_G(\boldsymbol{x}, \boldsymbol{x}')$ is the covariance function, which characterizes the correlation between different spatial locations.

In geological material parameters, exponential covariance model is commonly used, where variance and correlation lengths are specified through parametric forms. The 3D exponential covariance function can be expressed as:

$$C_G(\boldsymbol{x}, \boldsymbol{x}') = \sigma_G^2 \exp\left[-\left(\frac{|x-x'|}{l_x} + \frac{|y-y'|}{l_y} + \frac{|z-z'|}{l_z}\right)\right] \tag{6}$$

In Eq. (6), $\boldsymbol{x} = (x, y, z)$ and $\boldsymbol{x}' = (x', y', z')$ denote the spatial position vectors, σ_G^2 is the variance of the random field and represents the overall amplitude of fluctuation. The correlation lengths l_x, l_y, l_Z govern the degree of spatial smoothness along the three coordinate directions. Larger correlation lengths imply slower spatial variation in the corresponding direction, reflecting the inherent continuity of the geological medium.

Based on this covariance structure, the KLE represents the random field as a linear combination of deterministic spatial modes and independent random variables. By performing an eigen decomposition of the covariance function, one obtains the eigenvalues λ_i and the orthogonal eigenfunctions $\varphi_i(\boldsymbol{x})$, which satisfy:

$$\int_{\Omega_G} C_G(\boldsymbol{x}, \boldsymbol{x}')\varphi_i(\boldsymbol{x}')d\boldsymbol{x}' = \lambda_i \varphi_i(\boldsymbol{x}) \tag{7}$$

The random field can then be expressed as:

$$G(\boldsymbol{x},\omega) = \mu_G(\boldsymbol{x}) + \sum_{i=1}^{\infty} \sqrt{\lambda_i}\varphi_i(\boldsymbol{x})\xi_i(\omega) \tag{8}$$

In Eq. (8), $\xi_i(\omega)$ are uncorrelated standard random variables with zero mean and one variance.

The Eq. (8) shows that the spatial randomness of the field can be represented as a linear combination of deterministic spatial modes $\varphi_i(\boldsymbol{x})$ weighted by the random variables ξ_i. The magnitude of each eigenvalue λ_i indicates the contribution of the corresponding mode to the total variance. In practical computations, it is unnecessary to retain all modes, a accuracy approximation can be achieved by keeping the

first M dominant modes, replacing the ∞ in Eq. (8) with M. This truncation substantially reduces the stochastic dimensionality while preserving the essential statistical characteristics of the field. Within the PDEM, all uncertainties are represented by a finite set of basic random variables Θ. When structural or soil parameters exhibit spatial correlation, the truncated KLE variables ξ_i are incorporated into this basic variable set.

2.3 Kanai-Tajimi ground-motion model

In PDEM based probabilistic early-warning approaches for slope systems, the randomness of external excitation is a primary factor controlling the distribution of structural responses [27–28]. In practical engineering, it is often difficult to obtain a sufficient number of recorded earthquake motions to support statistical analysis. Therefore, synthetic ground motions generated from theoretical spectra are commonly used. These virtual ground motions are constructed to match the statistical characteristics of a target site and provide equivalent input for dynamic response analysis. Among various stochastic ground-motion models, the KT method is widely used in engineering seismology because it has proven suitable for reliability analyses of geotechnical and soil structure systems [29].

In the KT method, the ground acceleration is treated as filtered white noise passing through a linear single degree of freedom system representing the site layer [30–31]. Its power spectral density function is given by:

$$S_{KT}(\omega) = S_0 \frac{1+4\zeta^2\left(\omega/\omega_g\right)^2}{\left[1-\left(\omega/\omega_g\right)^2\right]^2+4\zeta^2\left(\omega/\omega_g\right)^2} \tag{9}$$

In Eq. (9), ω is the circular frequency (rad/s), $\omega_g=2\pi f_n$ is the dominant circular frequency, f_n is the dominant frequency (Hz), ζ is the bandwidth parameter, S_0 controls the overall energy level of the excitation.

The Eq. (9) represents the frequency response of a linear system under a unit white noise input, causing the spectrum to peak at $\omega=\omega_g$. A smaller ζ yields a sharper spectral peak. Synthetic acceleration time histories with this spectral shape are commonly generated using the Spectral Representation Method. After discretizing the frequency domain into N_f frequency points, a stationary stochastic acceleration process can be expressed as:

$$a_b(t) = \sum_{k=1}^{N_f} \sqrt{2S_{KT}\left(f_k\right)\Delta f}\cos\left(2\pi f_k t+\phi_k\right) \tag{10}$$

In Eq. (10), Δf is the frequency increment, taken as $1/t_n$, t_n is the duration of the process, ϕ_k are independent random phases uniformly distributed in $[0, 2\pi]$.

The generated process is stationary, with zero mean, constant variance, and a frequency distribution consistent with $S_{KT}(\omega)$. However, real earthquake motions are not stationary. Their energy evolves over time and typically exhibits an onset-growth-decay pattern. To capture this non-stationary characteristic, a time envelope function $E(t)$ is introduced. A commonly used exponential envelope is:

$$\begin{cases} E(t) = a\left(\dfrac{t}{t_n}\right)^b \exp\left(-c\dfrac{t}{t_n}\right) \\ c=\dfrac{b}{\varepsilon},\ a=\left(\dfrac{e}{\varepsilon}\right)^b,\ b=\dfrac{\ln T_r}{1-\dfrac{r}{\varepsilon}+\ln\dfrac{r}{\varepsilon}} \end{cases} \tag{11}$$

In Eq. (11), a, b, c control the amplitude, rise rate, and decay rate, respectively, ε denotes the relative time at which the energy peaks, T_r represents the ratio of the amplitude of the envelope at rt_n to the overall peak value, with $r \in [0,1]$ and typically $r = 0.9$.

Applying the envelope to the stationary process and rescaling yields a non-stationary acceleration time history consistent with the target ground-motion intensity:

$$\begin{cases} a_{\text{scaled}}(t) = \beta a(t) \\ a(t) = E(t)\,a_b(t) \\ \beta = \text{PGA}_{\text{target}} \Big/ \max_t \left|a(t)\right| \end{cases} \tag{12}$$

In Eq. (12), $\text{PGA}_{\text{target}}$ is the target peak ground acceleration (m/s^2), and β is the scaling factor.

2.4 Probabilistic monitoring and early-warning method

To achieve rapid updating of structural response distributions and risk identification while maintaining physical fidelity, computational efficiency, and online applicability, this study develops a five-step monitoring and early-warning framework that integrates PDEM and surrogate-based correction in Fig. 1. The workflow combines uncertainty modelling of

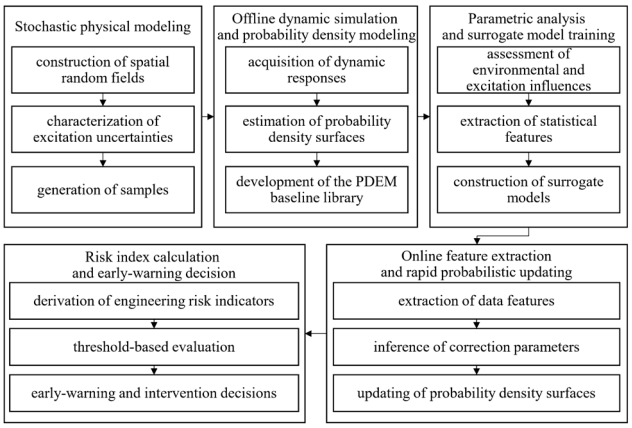

Fig. 1 Probabilistic monitoring and early-warning framework based on PDEM and surrogate model

geotechnical media and external excitations, offline construction of a probability database, parametric analysis of environmental factors, surrogate model training, and online correction and warning decision.

The first step involves physical modelling and definition of random variables. A dynamic model incorporating the geotechnical parameter, structural system, and external excitations is established, and their uncertainties are represented. Spatial variability of the geomaterial is modelled through random fields of key mechanical parameters such as elastic modulus, after KLE decomposition, a reduced set of random variables is retained to preserve dominant spatial correlations while reducing dimensionality. Excitation uncertainty is described using representative seismic or hydrodynamic inputs with sufficient variability in amplitude, phase, and duration. A sampling design is then constructed in the random variable space to generate training samples that cover space and excitation conditions.

The second step is offline simulation and PDEM baseline library construction. Dynamic numerical analyses are performed for all sampled realizations to obtain the time histories of the response quantities of interest. These responses are processed through the PDEM framework to compute the temporal evolution of the associated probability densities, yielding full PDSs. By organizing the PDSs corresponding to different features inputs, an offline PDEM database is established. This database serves as a statistical baseline during monitoring and provides essential data support for surrogate model development and subsequent online corrections.

The third step consists of parametric analysis and establishing of surrogate model. After constructing the database, further analyses are performed with respect to key environmental factors, such as excitation amplitude, water level, and scour depth, to quantify their influence on the statistics of the response. Representative statistical features extracted from these factors are paired with the distributional characteristics of the response to build datasets describing the input-output mapping. A surrogate model is then established to output distribution correction parameters conditioned on given environmental characteristics, thus replacing PDEM simulations with fast online corrections.

The fourth step is online feature extraction and rapid distribution correction. During monitoring, sensor data are collected at certain intervals or upon certain triggers, and real-time feature vectors are extracted and fed into the established surrogate model. The surrogate returns correction parameters that adjust the offline PDEM baseline and generate the current PDS. This process enables a direct and rapid mapping from real-time observations to probabilistic response characterization, avoiding repeated dynamic analyses and ensuring that uncertainty descriptions remain synchronized with monitoring data.

The fifth step involves extraction of risk indicators and warning decision. Based on the updated PDS, engineering-relevant risk metrics such as the distribution of peak responses, exceedance probabilities for specified thresholds, and indicators associated with failure criteria will be evaluated. Comparing these metrics with predefined risk thresholds enables automated warning or recommendations for manual inspection and refined analysis. In this manner, a probability-based monitoring-analysis-warning loop is established, supporting quantification of risk evolution and real-time decision-making capability.

The fourth step is online feature extraction and rapid distribution correction. During monitoring, sensor data are collected at certain intervals or upon certain triggers, and real-time feature vectors are extracted and fed into the established surrogate model. The surrogate returns correction parameters that adjust the offline PDEM baseline and generate the current PDS. This process enables a direct and rapid mapping from real-time observations to probabilistic response characterization, avoiding repeated dynamic analyses and ensuring that uncertainty descriptions remain synchronized with monitoring data.

The fifth step involves extraction of risk indicators and warning decision. Based on the updated PDS, engineering-relevant risk metrics such as the distribution of peak responses, exceedance probabilities for specified thresholds, and indicators associated with failure criteria will be evaluated. Comparing these metrics with predefined risk thresholds enables automated warning or recommendations for manual inspection and refined analysis. In this manner, a probability-based monitoring-analysis-warning loop is established, supporting quantification of risk evolution and real-time decision-making capability.

3 Π-shaped anti-scour wall slope

3.1 Numerical model construction

A river slope protected by the Π-shaped anti-scour wall is adopted as the numerical example. The geometry and structural configuration follow the design documentation: the wall height is 15 m, the sidewall thickness is 0.6 m, the top slab thickness is 0.5 m, and the concrete emergency blocks is 6 m wide and 2 m high in Fig. 2.

Numerical simulations are performed using FLAC3D. The concrete grades of the anti-scour wall, emergency

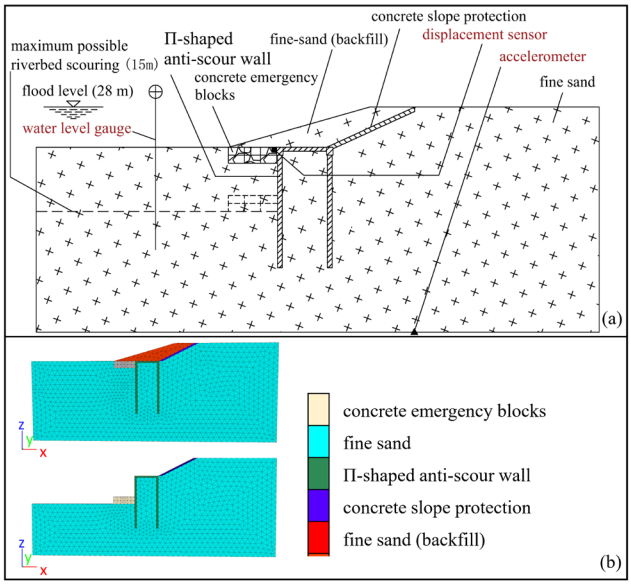

Fig. 2 Π-shaped anti-scour wall slope and monitoring-representative locations: (a) vertical section showing displacement gauge at wall top, accelerometer at model base, and river water-level indicator; (b) FLAC3D numerical model

blocks and slope protection are taken as C35, C25 and C25, respectively. The soil is represented by fine sand and fine sand (backfill). Mohr-Coulomb constitutive model is adopted to capture potential yielding and shear deformation. Material parameters are listed in Table 1. The model boundary conditions are defined by a free-field boundary at the base, viscous and free-field boundaries at the lateral sides, and pore-pressure loading to represent the water level. The response of interest is the horizontal relative displacement at the wall top with respect to the model base. A displacement monitoring point is arranged at the wall top front edge to represent wall-top horizontal movement, as would be measured by a displacement sensor. In addition, an acceleration monitoring point is defined at the model base to represent seismic input recording. A water-level gauge is also

Table 1 Material parameters

Material	C25	C35	Fine sand	Fine sand (backfill)
Density (kg/m^3)	2500	2500	2050	1620
Elastic modulus (MPa)	28	31.5	56 (0.25)	30
Poisson's ratio	0.2	0.2	0.3	0.3
Friction angle (°)	–	–	30	20
Cohesion (MPa)	–	–	0	0
Tensile strength (MPa)	–	–	0	0
Permeability (10^{-4}m/s)	–	–	1.16	1.16
Porosity	–	–	0.425	0.296

considered to represent river-stage variations, which correspond to pore-pressure boundary conditions in the numerical model. These monitoring-representative locations are illustrated in Fig. 2(a). In the modelling framework, the wall-top displacement serves as the primary response quantity for probabilistic characterization and updating. The base acceleration corresponds to measurable ground motion input, while river water level is introduced as hydraulic loading through the associated pore-pressure boundaries. Scour conditions are represented by variations in foundation elevation, corresponding to bed-level surveys commonly conducted in river engineering practice. These monitoring-representative quantities together define the data interface for PDEM analysis and surrogate-based probabilistic updating.

3.2 Uncertainty representation and excitation setting

To characterize the spatial variability of the fine sand, a 2D random field is constructed for the elastic modulus. Dimensionality reduction is performed using the KLE in Fig. 3. An anisotropic Gaussian covariance kernel is employed, with correlation lengths of 10 m and 5 m in the x- and z-directions, ignoring the z-direction differences. The prior mean and coefficient of variation reference the site investigation data. By balancing accuracy and computational cost, the first five dominant KLE modes are retained, forming a reduced random-variable subset that preserves the principal spatial heterogeneity.

The seismic excitation is generated according to the site class and regional design parameters specified in the seismic code for the project location. A target peak ground acceleration (PGA) of 0.20 g is adopted, corresponding to the design seismic intensity of the region, while the characteristic period (0.4 s) and bandwidth parameter (0.5) follow the site-specific response spectrum. Using the KT method, acceleration time histories consistent with the target spectrum are synthesized. To represent phase uncertainty, 30 curves with identical amplitude spectra but independent random phases are generated and assigned equal probability. A typical sample is shown in Fig. 4. Considering computational efficiency and the dominant structural response period, a uniform duration of 5 s is used.

Environmental conditions are defined based on design documentation, historical hydrological monitoring records, and engineering reports for the studied river section. Two representative water-level states are considered: normal operation and flood condition, reflecting seasonal variations and design-level high-water scenarios. These water-level states correspond to measurable river-stage variations and

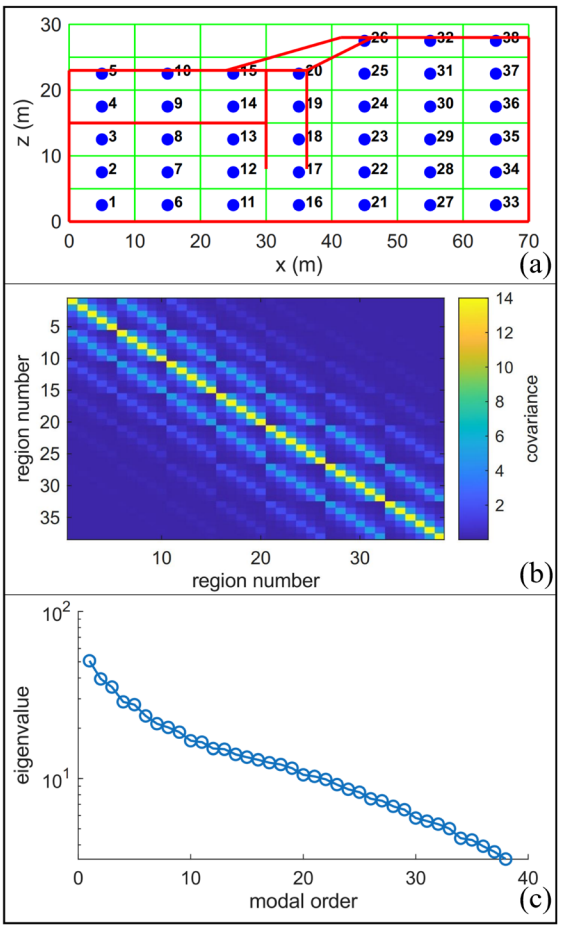

Fig. 3 KLE analysis: (a) fine sand region division; (b) covariance matrix of regions; (c) eigenvalue decay curve

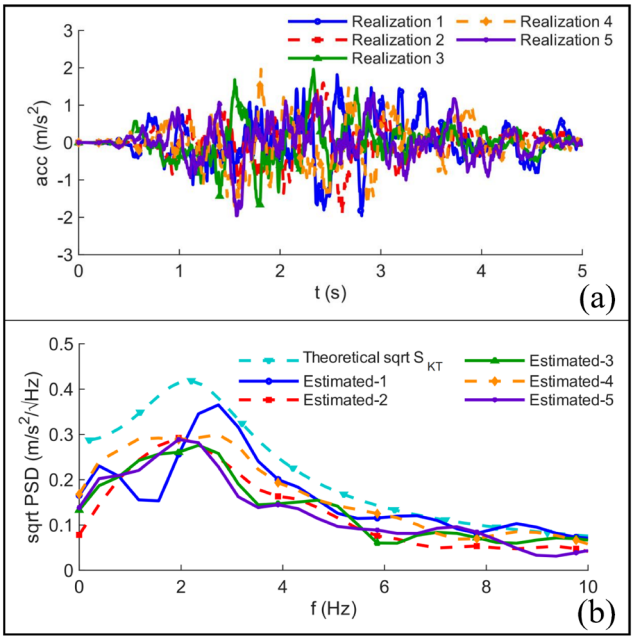

Fig. 4 KT seismic acceleration samples: (a) example time history; (b) spectral density estimate

are implemented in the model through pore-pressure boundary loading. Similarly, two scour states are introduced: no scour at elevation 23 m and maximum scour at elevation 15 m. The lower elevation represents a conservative estimate of foundation erosion under severe flow velocities according to engineering assessments. In practice, scour depth can be identified through periodic riverbed elevation surveys. By incorporating both no-scour and upper-bound scour scenarios, the model captures progressive foundation weakening effects. These environmental states are selected to span typical operational conditions as well as upper-bound extreme scenarios, ensuring adequate probabilistic coverage for baseline construction. Together with the stochastic material parameters and seismic samples, they form the complete set of scenarios required for establishing the offline PDEM baseline library.

3.3 Offline PDEM library construction

After defining the physical model and stochastic input scenarios, an offline sample set is generated. Deterministic dynamic analyses are conducted in FLAC3D for all samples, and the responses at the monitoring points are obtained. The probability density evolution method is then applied to compute the evolution surfaces of the response PDFs and relevant state variables.

The PDEM results across all environmental and stochastic combinations are systematically archived according to scenario labels, forming a structured offline PDEM library. This library serves as the statistical baseline for subsequent distribution correction and inference.

A parametric analysis is then performed to identify and quantify the influence mechanisms of environmental and excitation factors. Excitation intensity effects are investigated by scaling the acceleration amplitude while preserving waveform shape. Environmental effects are examined under different water level and scour conditions. Parametric correction relationships are extracted by comparing the PDEM outputs features across scenarios.

The extracted features consisting of environmental descriptors, excitation characteristics, and corresponding correction quantities are used to establish a surrogate model. With these inputs, the surrogate model predicts the correction parameters that adjust the baseline PDSs, enabling extrapolation from the finite offline samples to the scenario space.

During online deployment, the monitoring system extracts statistical features of the structural response within an observation window. These features are projected by the surrogate model into the parametric space, yielding correction

parameters. Combined with the offline PDEM database, they produce updated PDS at this window. This enables rapid transformation from measured data to evolving risk distributions, establishing a probability-based risk assessment and early-warning framework.

4 Results and analysis

4.1 Offline PDEM library establish and influencing factor analysis

The PDSs of the top horizontal relative displacement of the Π-shaped anti-score wall slope were analyzed under water levels of 23 m, 25 m, and 28 m, considering both no-scour and maximum scour conditions. The seismic acceleration peak was set to 0.2g, and the analysis accounted for spatial variability in fine sand elastic modulus and uncertainty in seismic phase. In total, six distinct combinations of water level and scour conditions were considered, with 30 sample realizations for each scenario. Each simulation obtained 5 s relative displacement time histories, which were then used to construct the corresponding probability density evolution surfaces and to extract statistical characteristics in Fig. 5, including mean and variance in Table 2.

As shown in Fig. 5, the probability distribution of the response changes over time, but it can also be observed that it has the characteristic of being concentrated. Both Fig. 5 and Table 2 indicate that scour significantly affects the PDE, increased scour leads to higher responses and larger variance, consistent with the theoretical reduction of soil anchorage under scouring. In contrast, variations in water level within the considered range exert a minor influence, slightly reducing the response due to the increased pore water pressure providing additional restraint. This analysis shows scour as a dominant factor influencing structural response, whereas water level has a comparatively smaller impact.

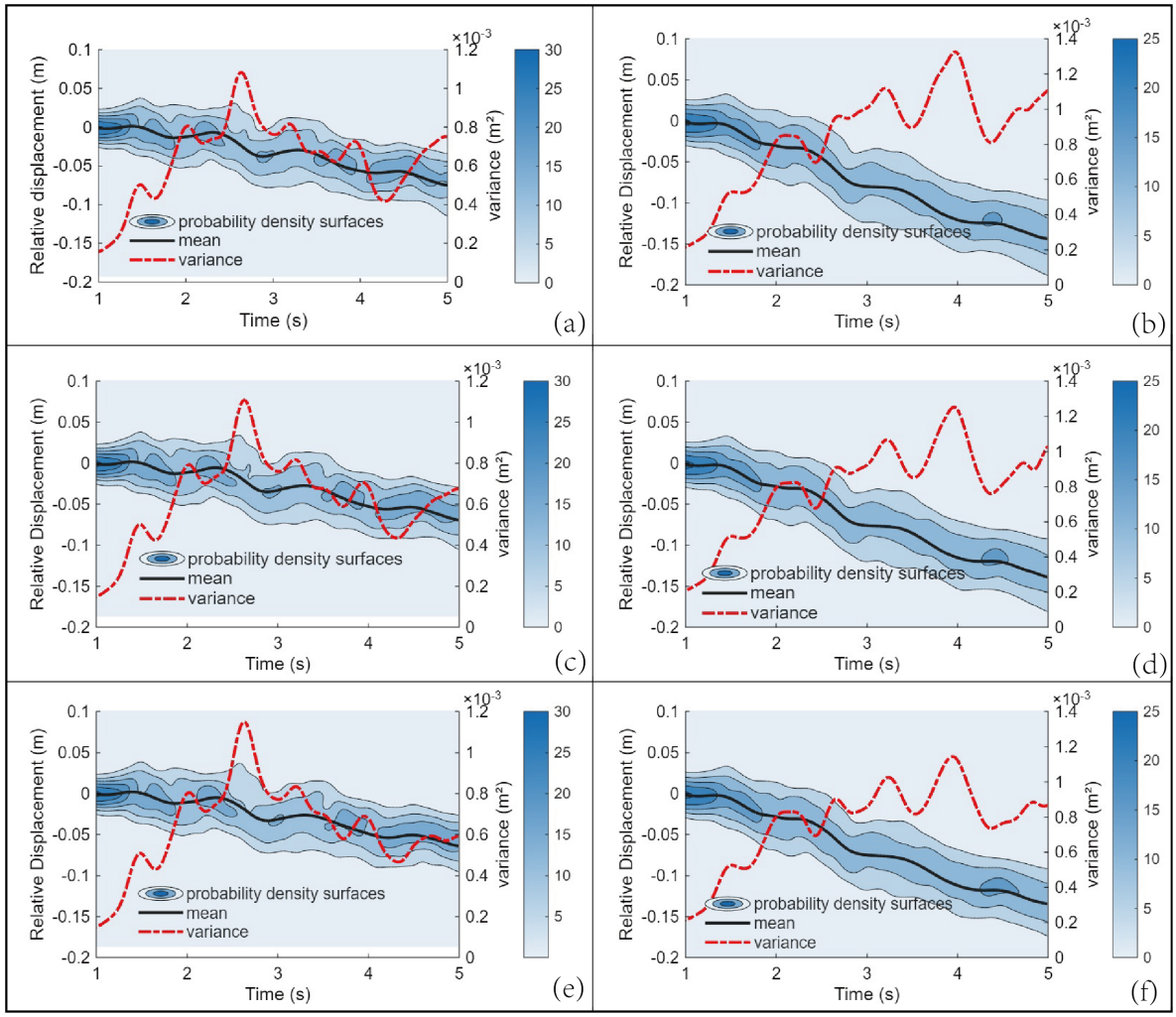

Fig. 5 PDSs of the relative horizontal displacement at the top of the anti-scour wall: (a) S1: no scouring at 23m water level; (b) S4: maximum scouring at 23m water level; (c) S2: no scouring at 25m water level; (d) S5: maximum scouring at 25m water level; (e) S3: no scouring at 28m water level; (f) S6: maximum scouring at 28m water level

Table 2 Time history characteristics of probability density surface

Analysis conditions	S1	S2	S3	S4	S5	S6
Maximum mean (m)	0.076	0.070	0.065	0.147	0.142	0.138
Variance	$6.4e^{-4}$	$5.7e^{-4}$	$5.0e^{-4}$	$1.2e^{-3}$	$1.1e^{-3}$	$9.9e^{-4}$

In practice, however, higher water levels often coincide with increased scour, necessitating consideration of both factors simultaneously.

To further quantify water level effects, 23 m water level was used as a reference, and response were evaluated at 25 m and 28 m for both no-scour and maximum scour scenarios. For each scenario, the 30 sample realizations were analyzed, and four response indicators were extracted, including peak displacement, root mean square, energy, and 90th percentile in Fig. 6(a) and (b). Relative scaling coefficients were computed with respect to the 23 m water level baseline, and a composite relative scaling coefficient was obtained by log averaging and median fitting in Fig. 6(c) and (d). For intermediate scour levels (18–23 m elevation), linear interpolation between the no-scour and maximum scour cases was used to estimate the composite scaling coefficient.

The influence of seismic peak acceleration on the response was also analyzed. Using a representative acceleration time history with a base peak of 0.2g, eleven scaled excitation levels (0.01–1.5 times the base peak) were simulated for both no-scour and maximum scour conditions. Fine sand properties were assumed homogeneous. The resulting 11 response time curves are shown in Fig. 7(a) and (b). Fig. 7(c) and (d) show that the response indicators exhibited an approximately quadratic relationship with the excitation coefficient.

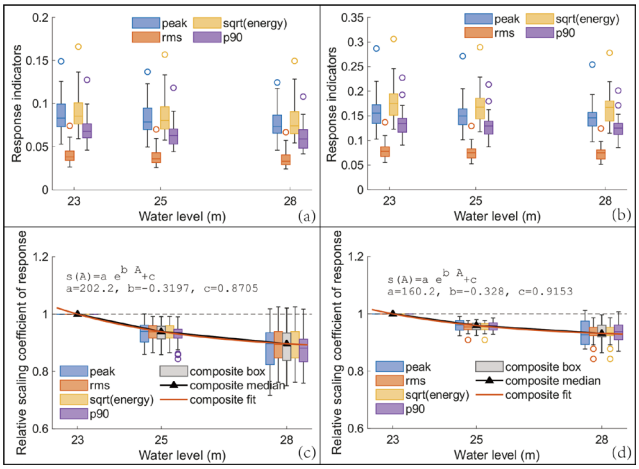

Fig. 6 Relationship between response relative scaling coefficient and water level: (a) sample without erosion; (b) sample with maximum erosion; (c) relationship without erosion; (d) relationship with maximum erosion

Composite relative scaling coefficients were obtained by log averaging across the indicators and fitted with a quadratic polynomial to establish functional relationships between peak acceleration and the response in Fig. 7(e) and (f). For practical scour conditions (18–23 m elevation), linear interpolation between no-scour and maximum scour results was applied to estimate the scaling coefficients.

4.2 Surrogate model construction and online probability density evolution reconstruction

Based on the previously presented analysis, a surrogate-based PDS model was developed by establishing functions between water level, seismic peak acceleration, and the interested physical quantity (top relative horizontal displacement of the anti-scour wall) under two conditions, no scour and maximum scour. Considering 5 s excitation time histories, the response PDEs for these two scenarios in Table 3 were obtained in Fig. 8. Supported by the offline PDEM library, the surrogate model enables near-real-time reconstruction of response feature uncertainty through parametric correction, providing a foundation for rapid online probability density updates. For validation, the surrogate model predictions were compared with direct PDEM calculations based on samples to assess accuracy in uncertainty characterization. Two representative scenarios, listed in Table 3, were selected for numerical verification, considering both soil randomness and seismic phase variability. Time histories and PDSs were analyzed and compared at both temporal and statistical levels.

For the selected scenarios, the response time histories and probability density evolution surfaces were first obtained from the PDEM simulations in Fig. 8(c) and (d). The surrogate model was then used to quickly reconstruct the PDEM evolution results in Fig. 8(e), and (f). Comparisons between Fig. 8(a) and (c), Fig. 8(b) and (d), show that under identical peak accelerations, the distributions of response time histories generated by new excitations closely match the corresponding PDSs in amplitude. This demonstrates that the surrogate constructed PDSs effectively preserve the main statistical features of the dynamic structural response and capture the variability induced by excitation uncertainty. Physically, this indicates that the PDSs not only encode the structure's response to external disturbances but also reflect the temporal evolution feature of uncertainty in the statistical distribution space. Moreover, the surrogate model allows direct extraction of time-varying means, variances, and extreme value distributions, providing a basis for defining probabilistic risk metrics. Compared with traditional warning systems

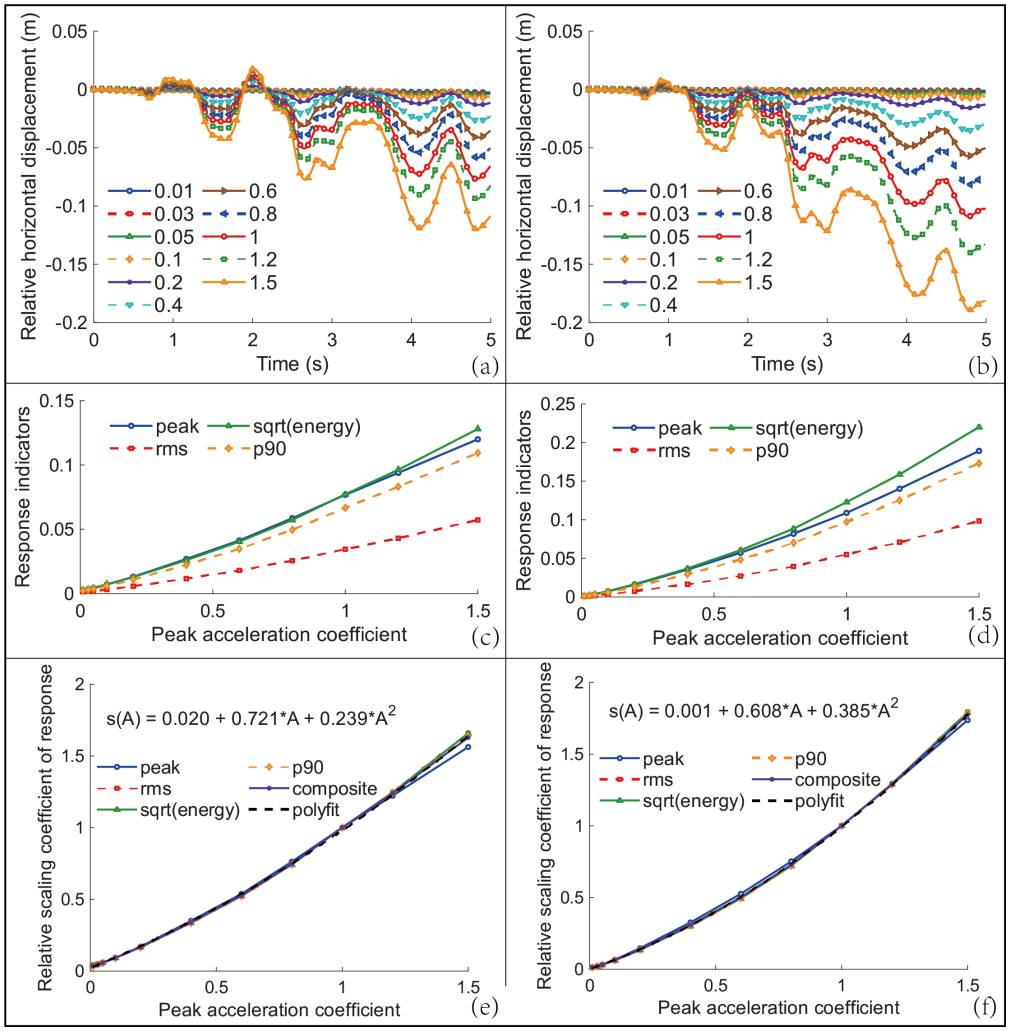

Fig. 7 Relationship diagram between relative scaling coefficient of response and peak acceleration coefficient: (a) time history of no erosion; (b) time history of maximum erosion; (c) no erosion sample; (d) maximum erosion sample; (e) no erosion relationship; (f) maximum erosion relationship

Table 3 Verification conditions

Analysis conditions	Water level	Peak excitation acceleration	Scour	Excitation duration
W_1	26m	0.05g	21m	5s
W_2	27m	0.1g	18m	5s

based on single value response, the PDEM approach simultaneously characterizes response magnitude and uncertainty trends, enabling more comprehensive dynamic warning.

Further comparisons between Fig. 8(c) and (e), Fig. 8(d) and (f), highlight the surrogate model's accuracy. The surrogate predicted PDSs closely reproduce the overall shape, peak location, major trends, and dynamic distribution of the PDEM results. To quantitatively evaluate the distribution differences, JSD and EMD were used as metrics, as shown in Fig. 8(g) and (h). Both metrics almost always remained below 0.1 for the two representative scenarios, indicating minimal statistical differences between surrogate predictions and PDEM computations. This confirms that the surrogate model can accurately capture the evolution of structural response uncertainty while significantly reducing computational cost.

Overall, the surrogate model reproduces both response amplitudes and distribution patterns consistent with PDEM results and maintains stability in representing time-varying uncertainties. Its core advantage lies in reducing high dimensional randomness to a real-time computable mapping, retaining the physical interpretability of the statistical behavior of structural dynamics. The surrogate predicted PDSs can further support warning systems based on confidence intervals, enabling early risk warnings. This probabilistic response prediction framework provides theoretical and practical feasibility for real-time monitoring and dynamic warning of similar hydraulic structures under complex environmental loads.

From an engineering perspective, the integration of surrogate models with PDEM provides an effective pathway for

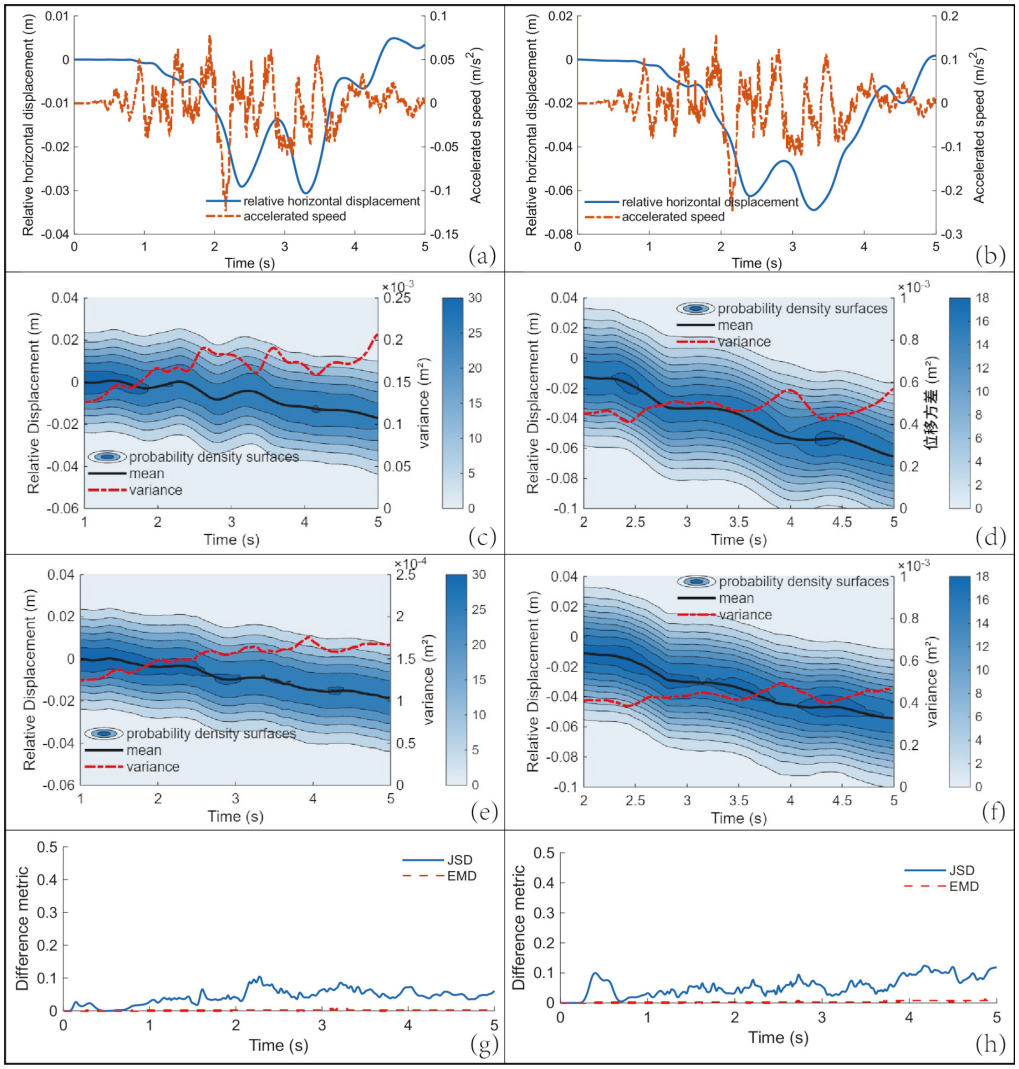

Fig. 8 PDS diagram of verification conditions: (a) excitation and response of W_1; (b) excitation and response of W_2; (c) simulation PDS of W_1; (d) simulation PDS of W_2; (e) deduction PDS of W_1; (f) deduction PDS of W_2; (g) difference between deduction and simulation of W_1; (h) difference between deduction and simulation of W_2

an edge-cloud collaborative monitoring system. Edge nodes perform data denoising, feature extraction, and surrogate model prediction to enable rapid risk identification, while the cloud handles high-cost parallel PDEM analyses, sample updates, and model rebuild. In summary, the proposed early-warning framework enables accurate approximation of PDEM results with significantly reduced computational cost, offering a scalable framework for structural response uncertainty analysis, probabilistic risk quantification, and real-time engineering decision-making.

5 Discussions

This study developed an early-warning framework that integrates PDEM and surrogate-based correction, and its applicability was demonstrated through a numerical case study of a Π-type anti-scour wall slope. The results indicate that KLE dimensionality reduction effectively captures the spatial randomness of geotechnical fields, transforming a high dimensional random field problem into a finite dimensional random variable problem and thereby significantly reducing the computational burden of PDEM analysis. Combined with the rapid correction method of the surrogate model, the framework enables near-real-time prediction of structural response feature while preserving the statistical structure of the distributions. This approach provides a pathway for structural health monitoring that balances computational efficiency and physical uncertainty, and demonstrates the feasibility of probabilistic early warning.

The truncation of KLE plays a key role in dimensionality reduction. By retaining the dominant modes, the main spatial variability of the random field can be captured with relatively low order expansions. However, when the geotechnical

medium exhibits strong heterogeneity or localized disturbances, low order truncation may introduce distortions in the response distributions. To mitigate this effect, increasing the truncation order can improve local accuracy, although this also increases the dimensionality of the random variables and the computational cost of PDEM. Compared with traditional Monte Carlo based statistical methods, the proposed framework demonstrates a clear advantage in balancing computational cost and accuracy. Nevertheless, in high-dimensional random variable settings, efficient sample selection and sensitivity analysis strategies remain necessary to identify the key factors contributing most to the response.

In the case study, typical environmental and excitation factors including water level, scour depth, and peak seismic acceleration were comprehensively considered. Comparative analysis shows that the surrogate model PDSs closely match direct PDEM computations, indicating generalizability under representative conditions. Unlike conventional studies that use deterministic responses as warning criteria, this framework derives time-varying mean and variance indicators from the probability density evolution process, allowing dynamic characterization of structural response uncertainty. Such distribution-based metrics provide recognition of potential instability trends, providing more information for monitoring systems.

Despite demonstrating robustness and computational efficiency, the framework has certain limitations. First, the excitation model generates equiprobable time histories using random phase synthesis, which does not fully account for variations in earthquake duration, spectral characteristics, or directional effects. These factors may cause bias in PDS under strong or long-period seismic excitations. Second, actual engineering systems may exhibit material layering, interface slippage, or nonlinear degradation, all of which could alter the response characteristics. Future work could incorporate multi-scale models that account for material damage evolution and interface interactions while maintaining computational feasibility, further improving the engineering applicability of probabilistic early-warning systems. From a practical implementation perspective, by integrating periodic validation and data reuse strategies, a dynamic, evolving monitoring loop can be established. Overall, the proposed framework offers a solution for uncertainty quantification in structural health monitoring, and holds potential for advancing the engineering application of probabilistic monitoring and early-warning systems for civil structures.

6 Conclusions

This study proposed an integrated probabilistic monitoring and early-warning framework that combines offline probability density evolution with online surrogate-based distribution correction. The framework enables near-real-time reconstruction of structural response probability distributions under spatially variable geotechnical conditions and stochastic excitations. The main findings can be summarized as follows:

1. The reduced-dimensional representation of spatial random fields effectively captures dominant geotechnical variability while maintaining computational feasibility for probability density evolution analysis. The resulting offline probability density surfaces provide a stable and physically interpretable baseline for probabilistic monitoring.
2. The surrogate-based correction strategy accurately reconstructs updated response distributions without repeated dynamic simulations. Quantitative comparison shows that the reconstructed probability density surfaces achieve distribution discrepancy metrics (Jensen-Shannon divergence and Earth Mover's Distance) generally below 0.1, while reducing computational cost by more than two orders of magnitude.
3. The framework enables extraction of time-varying mean, variance, and distribution-based risk indicators, allowing dynamic characterization of structural uncertainty beyond conventional threshold-based monitoring. This supports probability-informed early warning and decision-making for hydraulic structures.

Acknowledgement

The project presented in this article is supported by the National Science and Technology Major Project [2024ZD1700204, 2024ZD1004305], National Natural Science Foundation of China [52374113], and The Beijing Nova Program [20230484242].

References

[1] Li, Z., Langendoen, E. J., García, M. H. "Unveiling the Stochasticity of Bank Erosion: A Hybrid Deterministic and Stochastic Modeling Approach", Water Resources Research, 61(11), e2024WR039336, 2025. https://doi.org/10.1029/2024WR039336

[2] Gasser, E., Perona, P., Dorren, L., Phillips, C., Hübl, J., Schwarz, M. "A New Framework to Model Hydraulic Bank Erosion Considering the Effects of Roots", Water, 12(3), 893, 2020. https://doi.org/10.3390/w12030893

[3] Chi, F., Breul, P., Carvajal, C., Peyras, L. "Stochastic seepage analysis in embankment dams using different types of random fields", Computers and Geotechnics, 162, 105689, 2023. https://doi.org/10.1016/j.compgeo.2023.105689

[4] Chi, F., Carvajal, C., Breul, P., Peyras, L. "Reliability analysis of backward erosion piping in an embankment dam considering the spatial variability of soil properties", Scientific Reports, 15(1), 23974, 2025. https://doi.org/10.1038/s41598-025-09175-9

[5] Buijs, F. A., Hall, J. W., Sayers, P. B., Van Gelder, P. H. A. J. M. "Time-dependent reliability analysis of flood defences", Reliability Engineering & System Safety, 94(12), pp. 1942–1953, 2009. https://doi.org/10.1016/j.ress.2009.06.012

[6] Pol, J., Kanning, W., Jonkman, S. N., Kok, M. "Time-dependent reliability analysis of flood defenses under cumulative internal erosion", Structure and Infrastructure Engineering, pp. 1–17, 2024. https://doi.org/10.1080/15732479.2024.2416434

[7] Zhang, J. "Modern Monte Carlo methods for efficient uncertainty quantification and propagation: A survey", Wiley Interdisciplinary Reviews: Computational Statistics, 13(5), e1539, 2021. https://doi.org/10.1002/wics.1539

[8] Jin, S. S., Kim, G., Kwag, S., Eem, S. "Feasibility study of progressive Latin hypercube sampling and quasi-Monte Carlo simulation for probabilistic risk assessment", Geomatics, Natural Hazards and Risk, 15(1), 2425185, 2024. https://doi.org/10.1080/19475705.2024.2425185

[9] Weng, L. L., Yang, J. S., Chen, J. B., Beer, M. "Structural design optimization under dynamic reliability constraints based on probability density evolution method and quantum-inspired optimization algorithm", Probabilistic Engineering Mechanics, 74, 103494, 2023. https://doi.org/10.1016/j.probengmech.2023.103494

[10] Zhou, T., Guo, T., Dong, Y., Peng, Y. "Structural reliability analysis based on probability density evolution method and stepwise truncated variance reduction", Probabilistic Engineering Mechanics, 75, 103580, 2024. https://doi.org/10.1016/j.probengmech.2024.103580

[11] Huang, Y., Hu, H., Xiong, M. "Probability density evolution method for seismic displacement-based assessment of earth retaining structures", Engineering Geology, 234, pp. 167–173, 2018. https://doi.org/10.1016/j.enggeo.2018.01.019

[12] Huang, Y., Hu, H., Xiong, M. "Performance-based seismic fragility analysis of retaining walls based on the probability density evolution method", Structure and Infrastructure Engineering, 15(1), pp. 103–112, 2019. https://doi.org/10.1080/15732479.2018.1520906

[13] Luo, Y., Chen, J., Spanos, P. D. "Determination of monopile offshore structure response to stochastic wave loads via analog filter approximation and GV-GDEE procedure", Probabilistic Engineering Mechanics, 67, 103197, 2022. https://doi.org/10.1016/j.probengmech.2022.103197

[14] Lyu, M. Z., Chen, J. B. "A unified formalism of the GE-GDEE for generic continuous responses and first-passage reliability analysis of multi-dimensional nonlinear systems subjected to non-white-noise excitations", Structural Safety, 98, 102233, 2022. https://doi.org/10.1016/j.strusafe.2022.102233

[15] Wu, R. T., Jahanshahi, M. R. "Data fusion approaches for structural health monitoring and system identification: Past, present, and future", Structural Health Monitoring, 19(2), pp. 552–586, 2020. https://doi.org/10.1177/1475921718798769

[16] Hassani, S., Dackermann, U., Mousavi, M., Li, J. "A systematic review of data fusion techniques for optimized structural health monitoring", Information Fusion, 103, 102136, 2024. https://doi.org/10.1016/j.inffus.2023.102136

[17] Zhang, J., Zhang, K., Liu, P., Zhang, L., Fu, W., …, Yao, J. "Deep Bayesian surrogate models with adaptive online sampling for ensemble-based data assimilation", Journal of Hydrology, 649, 132457, 2025. https://doi.org/10.1016/j.jhydrol.2024.132457

[18] Li, J., Chen, J. B. "Stochastic Dynamics of Structure", John Wiley & Sons (Asia) Pte Ltd, 2009. ISBN 978-0-470-82424-5 Available at: http://refhub.elsevier.com/S0167-4730(22)00043-1/h0165 [Accessed: 20 December 2025]

[19] Chen, J., Yang, J., Li, J. "A GF-discrepancy for point selection in stochastic seismic response analysis of structures with uncertain parameters", Structural Safety, 59, pp. 20–31, 2016. http://dx.doi.org/10.1016/j.strusafe.2015.11.001

[20] Li J, Chen J B. "The probability density evolution method for dynamic response analysis of non-linear stochastic structures", International Journal for Numerical Methods in Engineering, 65(6), pp. 882–903, 2006. https://doi.org/10.1002/nme.1479

[21] Athapaththu, A. M. R. G., Tsuchida, T., Kano, S. "A new geotechnical method for natural slope exploration and analysis", Natural Hazards, 75(2), pp. 1327–1348, 2015. https://doi.org/10.1007/s11069-014-1384-0

[22] Srivastava, A., Babu, G. L. S. "Effect of soil variability on the bearing capacity of clay and in slope stability problems", Engineering Geology, 108(1), pp. 142–152, 2009. http://dx.doi.org/10.1016/j.enggeo.2009.06.023

[23] Karhunen K. "Über lineare Methoden in der Wahrscheinlichkeitsrechnung", Universitat Helsinki, pp. 3–79, 1947.

[24] Loève, M. "Fonctions aléatoires du second ordre" (title in english), In: Processus Stochastiques et Mouvement Brownien, Gauthier-Villars, 1948, pp. 299–352. (in French)

[25] Betz, W., Papaioannou, I., Straub, D. "Numerical methods for the discretization of random fields by means of the Karhunen–Loève expansion", Computer Methods in Applied Mechanics and Engineering, 271, pp. 109–129, 2014. http://dx.doi.org/10.1016/j.cma.2013.12.010

[26] Zhu, B., Hiraishi, T. "A decomposed Karhunen–Loève expansion scheme for the discretization of multidimensional random fields in geotechnical variability analysis", Stochastic Environmental Research and Risk Assessment, 38(4), pp. 1215–1233, 2024. https://doi.org/10.1007/s00477-023-02625-8

[27] Wang, Z., Zhang, Z., Dai, G., Zhou, Y., Cao, C., Su, T. "Reliability analysis of slopes reinforced by frame-anchor structures under earthquake conditions", Computers and Geotechnics, 177, 106885, 2025. https://doi.org/10.1016/j.compgeo.2024.106885

[28] Chen, Y., Baker, J. W. "Spatial Correlations in CyberShake Physics-Based Ground-Motion Simulations", Bulletin of the Seismological Society of America, 109(6), pp. 2447–2458, 2019. https://doi.org/10.1785/0120190065

[29] Song, L. F., Xu, B., Kong, X. J., Zou, D. G., Pang, R., Yu, X., Zhang, Z. "Three-dimensional slope dynamic stability reliability assessment based on the probability density evolution method", Soil Dynamics and Earthquake Engineering, 120, pp. 360–368, 2019. https://doi.org/10.1016/j.soildyn.2019.02.006

[30] Kanai, K. "Semi-empirical formula for the seismic characteristics of the ground", Bulletin of the Earthquake Research Institute, 35(2), pp. 309–325, 1957.

[31] Tajimi H. "A statistical method of determining the maximum response of a building structure during an earthquake", Proceedings of the 2nd World Conference on Earthquake Engineering, Tokyo, Japan, 1960, pp. 781–797.